Chinese Chemical Letters 33 (2022) 4317–4320

Contents lists available at ScienceDirect

Chinese Chemical Letters

journal homepage: www.elsevier.com/locate/cclet

Amidinium sulfonate hydrogen-bonded organic framework with fluorescence amplification function for sensitive aniline detection

Zhiwen Fan[1], Shihe Zheng[1], Hao Zhang, Kexin Chen, Yunbin Li, Chulong Liu*, Shengchang Xiang, Zhangjing Zhang*

Fujian Provincial Key Laboratory of Polymer Materials, College of Chemistry and Materials Science, Fujian Normal University, Fuzhou 350007, China

ARTICLE INFO

Article history:
Received 2 November 2021
Revised 1 January 2022
Accepted 6 January 2022
Available online 13 January 2022

Keywords:
Hydrogen-bonded organic frameworks (HOFs)
Charge-assisted hydrogen bonding
Fluorescence amplification
Aniline detection
Low detection limit

ABSTRACT

Although the construction of specific functional crystalline materials is still challenging, the multi-component molecular assembly has become a key solution for the design of functional materials. Here, we report a hydrogen-bonded organic framework (HOF) material FJU-360 constructed from disodium 6–hydroxy-5-[(4-sulfophenyl)azo]-2-naphthalenesulfonate (SSY) and terephthalimidamide. The charge-assisted hydrogen bonding between amidinium and sulfonate makes FJU-360 produce much stronger fluorescence than SSY, and can be used as a luminescence sensor to rapidly quench aniline through luminescence quenching. FJU-360 is sensitive and highly selective for the detection of aniline, and the detection limit reached 3.2 nmol/L, which is the lowest value reported currently. The mechanism of aniline response was analyzed through the aniline@FJU-360 single crystal structure, and the luminescence mechanism was clarified through density function theory calculations. This work is an important step towards the rational synthesis and assembly of sensing materials.

© 2022 Published by Elsevier B.V. on behalf of Chinese Chemical Society and Institute of Materia Medica, Chinese Academy of Medical Sciences.

As a key role in molecular assembly, hydrogen bonding leads to exciting supramolecular organizations such as organic molecular cages [1–3], polymers [4,5], and hydrogen-bonded organic frameworks (HOFs) [6–8]. The unique charge-assisted hydrogen bonding interaction formed by sulfonic acid and amine has been extensively explored to construct crystal network projects, such as *quasi*-hexagonal guanidinium organosulfonate roof (GS roof) [9–11], regular hexahedral hydrogen-bonded organic salts [12]. However, crystalline materials constructed by amidine and sulfonic acid is rarely reported and applied. Similar to guanidine, amidine will be protonated to form amidinium when reacting with sulfonic acid [13]. In addition to multiple hydrogen bonds, the association of the two also involves a favorable electrostatic force between the positive (dispersed on the amidinium group) and the negative (dispersed on the sulfonate group) charge [11]. This peculiar interaction is called “salt bridge” or charge-assisted hydrogen bond that can closely connect different building blocks [14]. Due to the effect of charge transfer, the bond length between the motifs is shortened. And a stronger H-bond with a shorter bond length is accompanied by better directivity (that is, a larger bond angle) [7]. From the perspective of rational design, compared with weak hydrogen bonds, highly oriented and strong hydrogen bonds help simplify the chemical process of self-assembly of organic molecules to expand the network [8].

Aniline plays an important role as an intermediate in chemical [15], pharmaceutical [16] and food industries [17]. Due to the influence of its own chemical and physical properties, it is easy to cause long-lasting environmental pollution. Aniline is easily to form a vapor, which enters the human body through the skin, digestive tract, and respiratory tract, and then resulting in anemia, toxic liver disease, and death in severe cases [18]. Although the traditional detection methods in analytical chemistry have low detection limits, high-performance liquid chromatography and gas chromatograph-mass spectrometer all require expensive instruments [19], long analysis time, and professional technical personnel [20].

In modern aniline detection technology, the colorimetric method and electrochemical method have more extensive results for the determination of aniline compounds, which are not suitable for trace analysis and specific analysis [21]. Although the instrument analyst is simple, the spectrophotometric method has low sensitivity, cumbersome operation, and interference large, many kinds of reagents are used, unstable and the used naphthalene ethylenediamine hydrochloride has the achilles heel of potential carcinogenic effects [22]. Therefore, low detection limit, high selectivity, and reversibility of aniline detection methods are very important for air pollution control, food safety testing, and medical

* Corresponding authors.
E-mail addresses: liucl@fjnu.edu.cn (C. Liu), zzhang@fjnu.edu.cn (Z. Zhang).
[1] These authors contributed equally to this work.

https://doi.org/10.1016/j.cclet.2022.01.009
1001-8417/© 2022 Published by Elsevier B.V. on behalf of Chinese Chemical Society and Institute of Materia Medica, Chinese Academy of Medical Sciences.

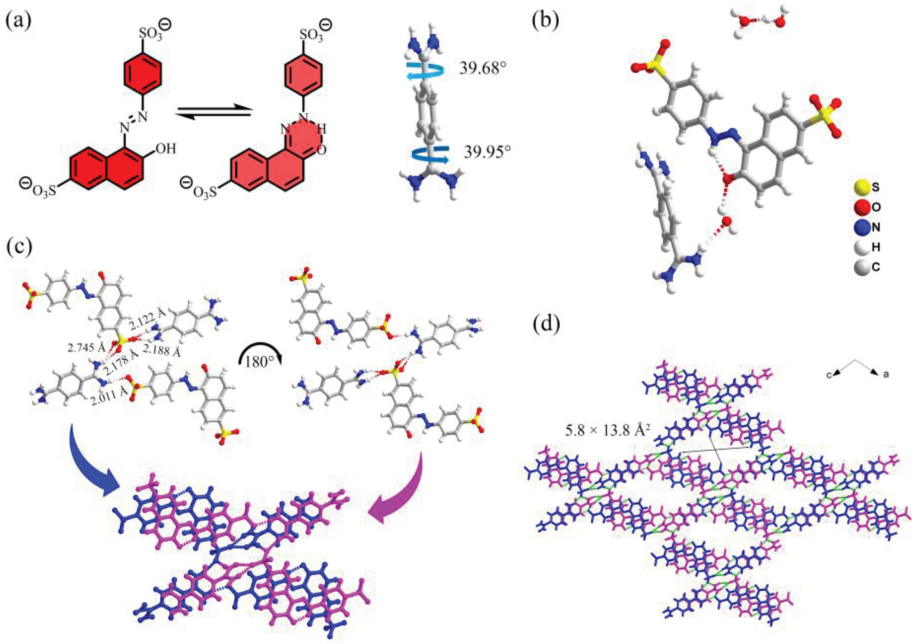

Fig. 1. (a) SSY undergoes tautomerism to form a planar structure (left) and the torsion angle formed by the two amidino groups of terephthalamidine and the benzene ring (right); (b) The simplest structure of FJU-360 unit; (c) Two SSY and two terephthalimidamides form tetramer layer by hydrogen bonds, and the two layers are superimposed in centrosymmetric by hydrogen bonds to form "X"-shaped column; (d) FJU-360 3D framework (hiding the guest molecule). Color code: S, yellow; C, gray; O, red; N, Blue; H, white.

diagnosis. With the continuous exploration in the field of materials, the good luminescence properties of metal-organic frameworks (MOFs) [23–25] and hydrogen-bonded organic frameworks (HOFs) [26,27] make them shine in aniline sensing and detection applications. These porous materials that achieve good fluorescence properties for aniline detection usually need to have suitable pores, better stability, and sites that can strongly interact with aniline.

In today's fluorescence sensing research, changes in luminous intensity (turned down or turned up) represent one of the easiest responses to analyte identification. Compared with turning on the counterpart, turning off fluorescence sensing is more susceptible to other quenchers or environmental stimuli, resulting in lower sensitivity and reliability [28,29]. In this work, we used charge-assisted hydrogen bonding to constructed a stable hydrogen-bonded organic framework material FJU-360, which is composed of disodium 6–hydroxy-5-[(4-sulfophenyl)azo]-2-naphthalenesulfonate (Sunset Yellow, abbreviate the anion to SSY) and terephthalimidamide. Interestingly, the transfer of electrons between SSY and terephthalimidamide makes FJU-360 show much stronger fluorescence than Sunset Yellow, and it shows an ultrasensitive response to aniline in ethanol, with a detection limit of 3.2 nmol/L. This response mechanism is unitary, and when there is interference from other aromatics, its impact can be ignored. Single crystal X-ray diffraction (SCXRD) measurements show that the deprotonated hydroxyl groups on the FJU-360 frame form hydrogen bonds with aniline molecules, which changes the electron cloud density of the frame and shrinks the crystal frame, show sensitive fluorescence sensing to aniline.

FJU-360 is a red needle-like crystal obtained by slowly evaporating the solvent at room temperature. SCXRD analysis shows that FJU-360 crystallizes in the orthogonal C2/C space group, and a unique three-dimensional (3D) framework is formed by hydrogen bonds assisted by SSY, terephthalimidamide, and water molecules through multiple charges (Fig. 1b). Viewed along the *b*-axis, in the 3D framework constructed by SSY and terephthalimidamide, SSY undergoes tautomerism to form a planar structure (Fig. 1a, left) [30], and the two amidinium group planes of terephthalimidamide form a torsion angle of 39.95° and 39.68° with the middle benzene ring (Fig. 1a, right), thus forming a tetramer structure constructed by two SSY and two terephthalimidamide ions. The five O•••H–N hydrogen bonds formed between sulfonate and amidinium groups are all in the range of 2.1 Å to 2.8 Å, indicate they are strong hydrogen bonds. These five hydrogen bonds can be divided into three categories, a double hydrogen bonds of 2.122 Å and 2.188 Å formed by the amidinium group and an oxygen atom of the sulfonate group on naphthalene; the other two oxygen atoms of the sulfonate group and one hydrogen atom of the amidinium group form a double hydrogen bonds with lengths of 2.178 Å and 2.745 Å; the sulfonate group on benzene and the amidinium group form a single heavy hydrogen bond with a length of 2.011 Å (Fig. 1c). Along the *b*-axis, every two centrally symmetrical tetramers are connected by two singlet hydrogen bonds with a length of 2.081 Å to form a one-dimensional (1D) "X"-shaped columnar structure (Fig. 1c). The bonding method between used tetramers is stacked to form a 3D HOF (Fig. 1d). FJU-360 has 1D diamond-shaped pores with a pore size of 5.8 × 13.8 $Å^2$. We tried to test the nitrogen adsorption after activation of the material to characterize the pore characteristics of the material. Unfortunately, FJU-360 has no nitrogen adsorption, and the framework collapses after losing the guest molecules because FJU-360 has a large pore size, does not have an interpenetrating structure, and has poor structural stability, water molecules act as a support framework in the pores (Fig. S3 in Supporting information), and the removal of guest molecules causes the pores collapsed.

Considering the exposed deprotonated oxygen atoms on the framework of FJU-360 may serve as binding site for aniline. Interaction between the guest molecules and the exposed sites on the framework may provide the feasibility for improving the sensitivity of aniline detection. Therefore, we tested the ability of FJU-360 to detect aniline in ethanol and the ability to sense other aromatic

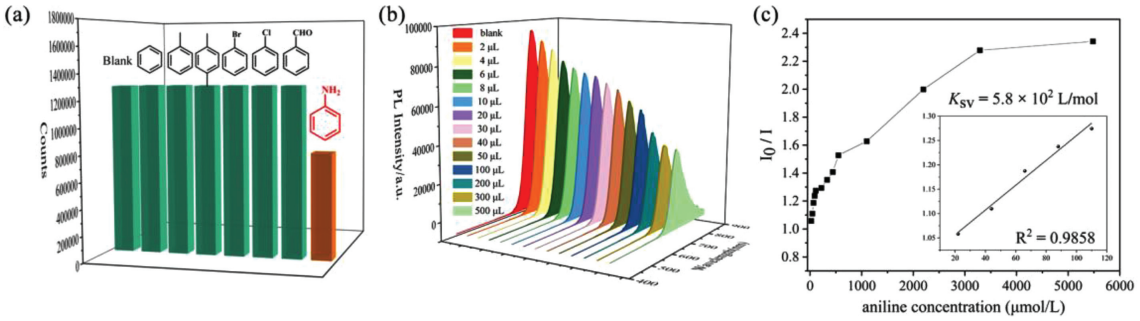

Fig. 2. (a) The change of fluorescence intensity of FJU-360 ethanol suspension after adding different analytes (5 μL analyte in 2 mL ethanol); (b) The luminescence of FJU-360 dispersed in different concentrations of aniline solution; (c) Stern-Volmer plot of FJU-360 I_0/I and aniline concentration in ethanol suspension.

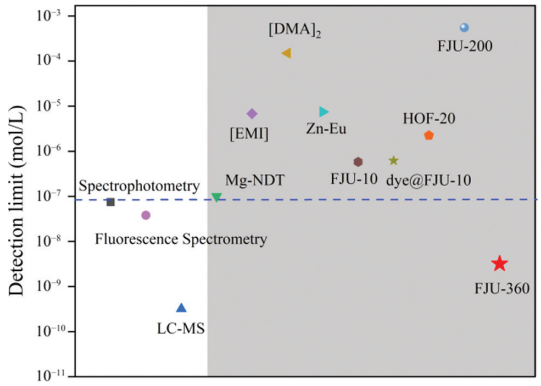

Fig. 3. Comparison of the detection limit of FJU-360 with other porous materials and instrumental analysis for the detection of aniline.

compounds with similar structures but different functional groups, including benzene, toluene, *p*-xylene, chlorobenzene, bromobenzene, and benzaldehyde. The test results indicate that FJU-360 has specific selectivity for aniline, all tested aromatic compounds have almost no effect on the fluorescence of FJU-360 except aniline (Fig. 2a). Subsequently, the fluorescence response of FJU-360 as a function of aniline concentration was quantitatively studied. The results show that as the concentration of aniline increases, the fluorescence intensity of the material gradually decreases (Fig. 2b). The quenching efficiency is calculated by the Stern-Volmer (SV) equation: $I_0/I = 1 + K_{SV}$ [M] (I_0/I is the ratio of fluorescence intensity before and after the addition of aniline, K_{SV} is the quenching constant (L/mol); [M] is the concentration of aniline in the experiment). The SV chart shows a good linear relationship between aniline and the fluorescence intensity of the sample at low concentrations (Fig. 2c). The deviation of the height curve with the concentration may be caused by the self-absorption phenomenon of the solution [31]. The quenching constant of FJU-360 reached 5.8×10^2 L/mol; the detection limit of FJU-360 reached 3.2 nmol/L calculated according to $3\sigma/k$ [32,33], which is the currently known minimum detection limit of aniline in porous materials (Fig. 3, Table S3 in Supporting information) [24–27,34–39].

The reusability of materials is an important indicator of FJU-360 in actual production and application. FJU-360 crystal can be reused only by immersing and cleaning in ethanol and water (v/v = 5:1). The fluorescence detection efficiency of regenerated FJU-360 for aniline is very close to the original sample (Fig. S6b in Supporting information), indicating that FJU-360 has good recyclability in sensing applications.

Solid-state emission fluorescence of Sunset Yellow and FJU-360 at room temperature shows that the fluorescence emission of FJU-360 at 645 nm is much stronger than that of Sunset Yellow, which may be due to the intra- and inter-molecular proton transfer and electron transfer [40,41]. Through density functional theory (DFT) calculation and analysis of the double dipole part composed of two SSY and two terephthalimidamide in FJU-360, it is found that electron transfer occurs between SSY and terephthalimidamide. The highest occupied orbital energy calculated by SSY as a theoretical calculation is −4.85 eV, the theoretically calculated lowest occupied orbital is on terephthalimidamide with −4.60 eV (Fig. 4c). When electrons return from LUMO to HOMO, strong fluorescence is generated.

To explore the mechanism of FJU-360 fluorescence sensing in-depth, we used SCXRD technology to determine the precise structure of FJU-360 treated with aniline. Aniline@FJU-360 is obtained by immersing FJU-360 crystal in aniline solution through the single crystal to single crystal structure conversion. In aniline@FJU-360, the aniline molecule replaced two guest water molecules in FJU-360 channel and distributed in the two corners of the parallelogram channel, which can be well-identified (Fig. 4a). The amino group of the aniline forms a hydro-gen bond with a bond length of 2.426 Å with the exposed O atom in the pore (Fig. 4b). Aniline is a good electron donor, and SSY is a good electron acceptor when it undergoes tautomerization into quinone. The hydrogen bond between aniline and the framework changes the distribution of electron cloud density. Through DFT calculations, it is found that energy difference between the HOMO and LUMO orbitals before and after the action of the aniline molecule increases to 1.8 times (Fig. 4c) [42], the calculation results also show that the charge transfer of FJU-360 occurs between terephthalimidamide and SSY, while the electron transfer of aniline@FJU-360 occurs between terephthalimidamide and aniline. The decrease in electron cloud density leads to an increase in the anti-bond orbital energy, thereby reducing fluorescence of FJU-360.

In a word, we used SSY and terephthalimidamide as building blocks successfully synthesized a 3D HOF FJU-360 by charge-assisted hydrogen bonding. FJU-360 exhibits much stronger fluorescence than SSY and has the potential for rapid response and highly selective detection of aniline. The detection limit reached 3.2 nmol/L, which is the lowest value currently reported among porous materials. Single crystal X-ray diffraction measurements and density functional theory calculations show that FJU-360 interacts with aniline through the exposed oxygen atoms in the pores as the binding site, which reduces the electron cloud density of the framework and reduces the fluorescence of the material. The use of charge-assisted hydrogen bond construction in the mode of crystalline functional materials enriches crystal network engineering and provides new ideas for the design of functional materials for multi-component molecular assembly. At the same time, reusability, low detection limit, and high quenching constant K_{SV}

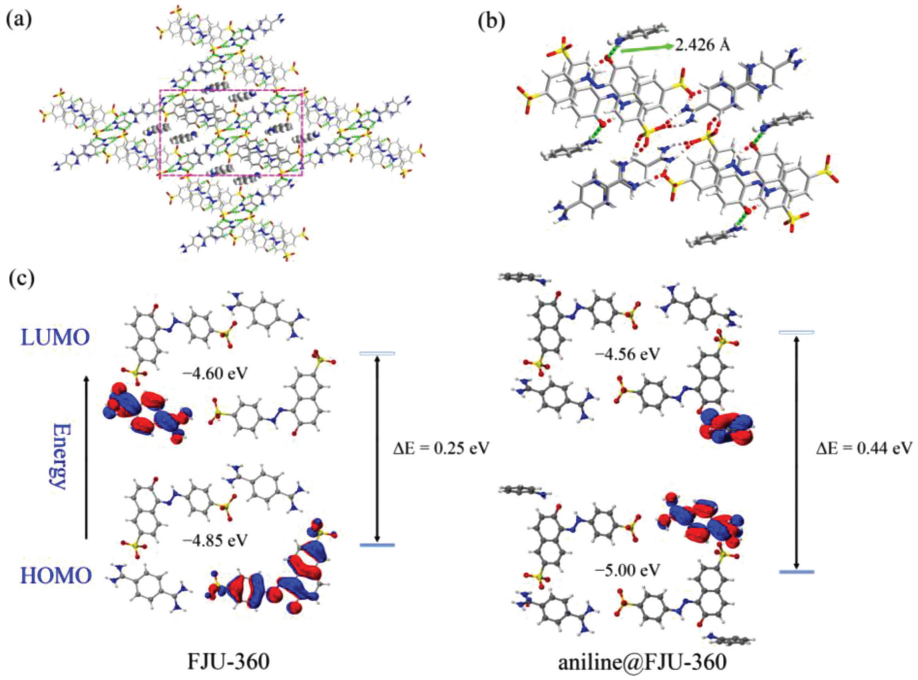

Fig. 4. (a) Aniline adsorption sites in FJU-360 (selected fragments are highlighted); (b) Hydrogen bonding between aniline and oxygen atom on the inner wall of FJU-360 channels; (c) Calculated FJU-360 and aniline@FJU-360 selected fragment energy level difference diagram based on DFT at the b3lyp/631+g(d,p) basis set. The oxygen in the inner wall of the pore as the action site and the aniline form a hydrogen bond of 2.426 Å, which makes the activation energy of FJU-360 from HOMO to LUMO reach 0.44 eV.

make FJU-360 promising for aniline detection, and may lead to important potential applications as a functional material in the fields of industry, agriculture, medicine, and environmental systems.

Declaration of competing interest

The authors declare that they have no known competing financial interests or personal relationships that could have appeared to influence the work reported in this paper.

Acknowledgments

This work was supported by the National Natural Science Foundation of China (Nos. 21673039, 21573042, 21805039, 21975044, 21971038 and 21922810), and the Fujian Provincial Department of Education (No. JAT200077).

Supplementary materials

Supplementary material associated with this article can be found, in the online version, at doi:10.1016/j.cclet.2022.01.009.

References

[1] T. Hasell, A.I. Cooper, Nat. Rev. Mater. 1 (2016) 1–14.
[2] H. Wang, Y. Jin, N. Sun, W. Zhang, J. Jiang, Chem. Soc. Rev. 50 (2021) 8874–8886.
[3] G.A. Leith, C.R. Martin, J.M. Mayers, et al., Chem. Soc. Rev. 50 (2021) 4382–4410.
[4] H. Sun, Y. Liang, M.P. Thompson, N.C. Gianneschi, Prog. Polym. Sci. (2021) 101427.
[5] C.J. Reese, S.G. Boyes, Prog. Polym. Sci. 114 (2021) 101361.
[6] I. Hisaki, C. Xin, K. Takahashi, T. Nakamura, Angew. Chem. Int. Ed. 58 (2019) 11160–11170.
[7] R.B. Lin, Y. He, P. Li, et al., Chem. Soc. Rev. 48 (2019) 1362–1389.
[8] B. Wang, R.B. Lin, Z. Zhang, S. Xiang, B. Chen, J. Am. Chem. Soc. 142 (2020) 14399–14416.
[9] A. Karmakar, R. Illathvalappil, B. Anothumakkool, et al., Angew. Chem. Int. Ed. 55 (2016) 10667–10671.
[10] V.A Russell, M.C. Etter, M.D. Ward, J. Am. Chem. Soc. 116 (1994) 1941–1952.
[11] Y. Li, M. Handke, Y.S. Chen, et al., J. Am. Chem. Soc. 140 (2018) 12915–12921.
[12] A. Yamamoto, T. Hirukawa, I. Hisaki, M. Miyata, N. Tohnai, Tetrahedron Lett. 54 (2013) 1268–1273.
[13] Z.P. Deng, L.H. Huo, H. Zhao, S. Gao, Cryst. Growth Des. 12 (2012) 3342–3355.
[14] L. Pop, N.D. Hadade, A. van der Lee, et al., Cryst. Growth Des. 16 (2016) 3271–3278.
[15] B.G. Soares, G.S. Amorim, F.G. Souza Jr, M.G. Oliveira, J.P. da Silva, Synth. Met. 156 (2006) 91–98.
[16] A. Grirrane, A. Corma, H. García, Science 322 (2008) 1661–1664.
[17] V. Alagarsamy, V.R. Solomon, K. Dhanabal, Bioorg. Med. Chem. 15 (2007) 235–241.
[18] R. Benigni, L. Passerini, Mutat. Res. Rev. Mutat. 511 (2002) 191–206.
[19] W. Stillwell, M.S. Bryant, J.S. Wishnok, Biomed. Environ. Sci. 14 (1987) 221–227.
[20] S. Pandey, K.K. Nanda, ACS Sensors 1 (2016) 55–62.
[21] Y. Zhang, C. Peng, X. Ma, Y. Che, J. Zhao, Chem. Commun. 51 (2015) 15004–15007.
[22] Z. Quan, G. Xie, Q. Peng, et al., Pol. J. Environ. Stud. 25 (2016) 1669.
[23] Y. Chen, B. Wang, X. Wang, et al., ACS Appl. Mater. Interfaces 9 (2017) 27027–27035.
[24] L. Li, J.Y. Zou, S.Y. You, et al., Dalton Trans. 46 (2017) 16432–16438.
[25] L. Liu, Z. Yao, Y. Ye, et al., ACS Appl. Mater. Interfaces 11 (2019) 16490–16495.
[26] B. Wang, R. He, L.H. Xie, et al., J. Am. Chem. Soc. 142 (2020) 12478–12485.
[27] Z. Ke, K. Chen, Z. Li, et al., Chin. Chem. Lett. 32 (2021) 3109–3112.
[28] I. Hisaki, Y. Suzuki, E. Gomez, et al., J. Am. Chem. Soc. 141 (2019) 2111–2121.
[29] T. Liu, B. Wang, R. He, et al., Can. J. Chem. 98 (2020) 352–357.
[30] W. Xiao, C. Hu, D.J. Carter, et al., Cryst. Growth Des. 14 (2014) 4166–4176.
[31] Z. Han, K. Wang, Y. Guo, et al., Nat. Commun. 10 (2019) 5117.
[32] L. Liu, Y. Wang, R. Lin, et al., Dalton Trans. 47 (2018) 16190–16196.
[33] G. He, H. Peng, T. Liu, et al., J. Mater. Chem. 19 (2009) 7347–7353.
[34] A. Zhang, L. Jia, Spectrosc. Spect. Anal. 24 (2004) 723–725.
[35] C.Y. Zhou, C.Y. Luo, H.J. Yu, et al., Chin. J. Anal. Chem. 44 (2016) 935–941.
[36] W. Humphrey, A. Dalke, K. Schulten, J. Mol. Graphics 14 (1996) 33–38.
[37] A. Mallick, B. Garai, M.A. Addicoat, et al., Chem. Sci. 6 (2015) 1420–1425.
[38] H.J. Feng, L. Xu, B. Liu, H. Jiao, Dalton Trans. 45 (2016) 17392–17400.
[39] X.L. Huang, L. Liu, M.L. Gao, Z.B. Han, RSC Adv. 6 (2016) 87945–87949.
[40] Z. Han, W. Shi, P. Cheng, Chin. Chem. Lett. 29 (2018) 819–822.
[41] Y. Guo, Z. Han, H. Min, et al., Inorg. Chem. 60 (2021) 9192–9198.
[42] A.A. Velikorodnyi, E.I. Morosanova, J. Anal. Chem. 55 (2000) 1105–1110.